Open Science Journal of Statistics and Application
2014; 2(1): 10-16
Published online February 28, 2014 (http://www.openscienceonline.com/journal/osjsa)

Probability neural network classification model of brain tissue pathologies using high frequency techniques

S. S. Shanbhag[1, *], G. R. Udupi[1], K. M. Patil[2], K. Ranganath[3]

[1]Electronics and Communication Engineering, Gogte Institute of Technology, Belgaum, India
[2]Indian Institute of Technology (Madras), Belgaum, India
[3]RAGAVS, Diagnostics and Research Center Pvt. Ltd., Bangalore, India

Email address

supriya_sp@yahoo.com (S. S. Shanbhag)

To cite this article

S. S. Shanbhag, G. R. Udupi, K. M. Patil, K. Ranganath. Probability Neural Network Classification Model of Brain Tissue Pathologies using High Frequency Techniques, *Open Science Journal of Statistics and Application.* Vol. 2, No. 1, 2014, pp. 10-16.

Abstract

The conventional method of analysing the brain tissue pathologies on Diffusion Weighted-Magnetic Resonance (DW-MR) images is by human inspection. Such operator-assisted classification techniques are not viable for large amounts of medical data and are generally non-reproducible. The use of neural networks shows a great potential in this area to carry out fast, accurate and automatic data classification. In the present study, Probability Neural Network (PNN) architecture was employed to develop an automated classification model based on the quantified signal intensity variations on DW-MR images, derived from the subjects with brain pathologies, using High Frequency Power (HFP) parameter. The PNN models were designed to provide important reference in judging the timing and developmental stages of the subjects with cerebral infarction and Intracerebral Haemorrhage (ICH), and help in carrying out the differential diagnosis of the subjects with brain tumors, namely, glioma and meningioma. The PNN models were able to accurately (100%) categorize ICH subjects into their respective stages, and presented an overall efficiency of 96.67% in classifying the infarct subjects. Also the model was able to clearly differentiate (100%) between the subjects with glioma and meningioma. Consequently, the PNN models developed in the present work were helpful in providing valuable information about the brain tissue pathologies, which could speed up the diagnosis and execution of treatment. Further, it could help in providing timely and appropriate treatment to the subjects with these brain pathologies, to protect them from additional damage to their brain tissues.

Keywords

Cerebral Infarction, Diffusion Weighted Images, Glioma, Intracerebral Haemorrhage, Magnetic Resonance Imaging, Meningioma, Probability Neural Network, Signal Intensity

1. Introduction

Automated classification in medical images is motivated by the need of high accuracy when dealing with a human life. Also, computer assistance is demanded in medical organizations due to the fact that it could improve the results of humans, so that false negative cases are kept at a very low rate [1]. Conventional methods of monitoring and diagnosing brain tissue pathologies rely on detecting the presence of particular features, by a human observer. Due to large number of patients several techniques for automated diagnostic systems have been developed in recent years to attempt to solve this problem. Such techniques work by transforming the mostly qualitative diagnostic criteria into a more objective quantitative feature classification problem [1]. Various kinds of neural network architectures including MultiLayer Perceptron (MLP) neural network, Radial Basis Function (RBF) neural network, Self-Organizing Map (SOM) neural network and Probability Neural Network (PNN) have been proposed [2] to classify patterns based on learning from examples. Different neural network

paradigms employ different training rules, but all in some way determine pattern statistics from a set of training samples, and then classify new patterns on the basis of these statistics [3]. However, because of ease of training and a sound statistical foundation in Bayesian estimation theory, PNN has become an effective tool for solving many classification problems [3-5]. The main advantages that discriminate PNN are fast training process, an inherently parallel structure, guaranteed to converge to an optimal classifier as the size of the representative training set increases, and training samples can be added or removed without extensive retraining [6].

The purpose of the present work was to devise an automated brain tissue pathology classification model, by using prior information about the signal intensity characteristics of the brain pathology on Diffusion Weighted-Magnetic Resonance (DW-MR) images of the human brain. The evolution/appearance of the signal intensity characteristics on DW-MR images of the brain in the axial plane were analysed to identify the different levels of changes taking place in the subjects with the brain tissue pathologies, namely, *cerebral infarction*, *Intracerebral Haemorrhage* (*ICH*) and *brain tumors* (*glioma* and *meningioma*). An effort was made to grade the signal intensity variations on DW-MR images using High Frequency Power (HFP) values. The HFP values derived from the pathology side were compared to the corresponding HFP values obtained from the respective contralateral normal hemispheres of the subjects. Further, quantitative brain pathology PNN models were developed using the HFP parameter that were employed to automatically classify the stages of cerebral infarction [7], categorize the stages of ICH [8], and differentiate between the types of brain tumors (glioma and meningioma). The PNN models developed in the present work could positively be employed to derive valuable information about the particular brain tissue pathology, which may possibly assist the medical personnel in the speedy diagnosis and execution of treatment. Further, the proposed computer based technique would simplify the estimation process and provide information essential for the further management and therapeutic decisions, even in the absence of a medical expert.

2. Materials and Methods

2.1. Clinical Data and Diffusion Weighted Imaging

The clinical data in the present study is obtained from 'RAGAVS' Diagnostic and Research Center, Bangalore, India, and Vikram Hospital, Bangalore, India. The ethics approval is obtained from the committee of clinical research at the 'RAGAVS' Diagnostic and Research Center, and Vikram Hospital, to carry out the investigations on the clinical data provided. Applying the clinical inclusion criteria, we identified 98 cases with clinically definite cerebral infarctions with known symptom onset, which were employed in training and testing the PNN model. This population consisted of 64 male and 34 female subjects, ranging in age from 25 to 95 years (mean, 62.87 years). Diffusion Weighted - Magnetic Resonance Imaging (DW-MRI) examinations were performed on 24 subjects within 24 hours of symptom onset; 15 subjects between days 1 and 4; 38 subjects between days 5 and 9; 12 subjects between days 10 and 14; and 09 subjects after day 15.

Among all the ICH subjects admitted, we retrospectively selected 42 cases that showed isolated ICH without the presence of underlying tumor or infarction on initial radiologic and follow-up examinations, which were employed in training and testing the PNN model. This population consisted of 29 male and 13 female subjects, ranging in age from 28 to 85 years (mean, 58.62 years). DW-MRI examinations were performed on 09 subjects within 24 hours of symptom onset; 05 subjects between days 1 and 7; 15 subjects between days 7 and 14; and 13 subjects after 14 days.

Findings of DW-MRI examinations performed on 22 cases (15 male, 07 female; mean age, 56.55 years; age range, 39 – 83 years) with clinically proved glioma and 12 cases (04 male, 08 female; mean age, 56.50 years; age range, 26 – 81 years) with clinically proved meningioma, were also retrospectively selected, and employed in training and testing the PNN model.

All the subjects underwent clinical Magnetic Resonance (MR) imaging with 1.5 Tesla symphony maestro class MR scanning system from Siemens. DW-MRI was performed by using a multisection, single-shot, spin-echo, echo-planar pulse sequence with following parameters: Repetition Time [TR] = 3200 ms, Echo Time [TE] = 94 ms, acquisition matrix = 128 x 128, Field of View [FOV] = 230 mm x 230 mm, and diffusion gradient value of b = 1000 s/m^2 along 19 axial slices, 5 mm thick slice and intersection gap of 1.5 mm.

2.2. Signal Intensity High Frequency Power

DW-MRI makes it to visualize and measure the altered rates of water diffusion, by producing a bright imaging appearance in the area of the brain, affected by pathology [9, 10]. Consequently, on examining the spatial intensity variation distribution on DW-MR images for the subjects with brain pathology, it is observed that the signal intensity is not uniformly distributed over the entire DW-MR image. There are abrupt jumps in the signal intensity, in the area of pathology, in contrast to the other healthy areas of the brain, where the signal intensity distribution is almost uniform [8, 11-14]. Exploring the power spectrum of the DW-MR intensity image for these subjects would thereby result in a higher value for the higher spatial frequency power component out of the total power spectrum, in the area of brain pathology. In contrast, the higher spatial frequency power component on the contralateral normal hemisphere (mirror image) of the same subject is considerably low. Consequently, the HFP value in the area of brain pathology is much elevated in comparison to the HFP value on the contralateral normal hemisphere of the same subject.

Consider an input image, *f(x, y)*, corresponding to an image size represented by (M x N) pixels. The Fourier spectrum, *F(u, v)*, of the image, *f(x, y)*, is evaluated. The spatial frequencies and their distribution are analysed by performing the two-dimensional Discrete Fourier Transform (DFT) using MATLAB version 7.7. The spatial frequencies (*u* and *v*) are denoted by cycles per pixel, since the image size (distance) for the analysis is given in terms of pixels. Using the periodicity property of DFT [15], the Fourier spectrum is shifted to the center of the frequency plane. The DC component, *F(0, 0)*, is deleted, since it gives only the average value of the image intensity. The power spectrum is obtained by squaring the magnitudes of the Fourier spectrum signal intensity variations [15, 16] of the DW-MR image. The total power (*TP*), in the image is obtained using Eq. 1. Since the values of M and N are different (depend on the size of the particular region of the brain), the cut-off frequency, D_0 (in cycles per pixel), which separates the lower and higher spatial frequency components (as shown in Fig. 1), is defined by Eq. 2.

$$TP = \left\{ \sum_{u=-\frac{M}{2}}^{\frac{M}{2}} \sum_{v=-\frac{N}{2}}^{\frac{N}{2}} \left| F(u,v) \right|^2 \right\} - \left| F(0,0) \right|^2 \tag{1}$$

$$D_0 = \begin{cases} \dfrac{M}{4} & if \quad N \geq M \\ \dfrac{N}{4} & if \quad N < M \end{cases} \tag{2}$$

D(u, v) is the distance from the point *(u, v)* to the origin of the frequency plane, defined by Eq. 3.

$$D(u,v) = \sqrt{u^2 + v^2} \tag{3}$$

The Low Frequency Power (*LFP*) and *HFP* are calculated using Eq. 4 and 5 respectively.

$$LFP = \left\{ \sum_{D(u,v)=0}^{D_0} \left| F(u,v) \right|^2 \right\} - \left| F(0,0) \right|^2 \tag{4}$$

$$HFP = TP - LFP \tag{5}$$

The HFP value evaluated in the area of brain pathology is compared to the corresponding HFP value on the contralateral normal hemisphere of the same subject, to obtain the relative signal intensity HFP (RHFP) value. The RHFP value given by Eq. 6 is quantified across different subjects diagnosed with the brain pathology. RHFP value is employed in differentiating pathology tissues from healthy tissues and further used in deriving useful information about the brain pathology.

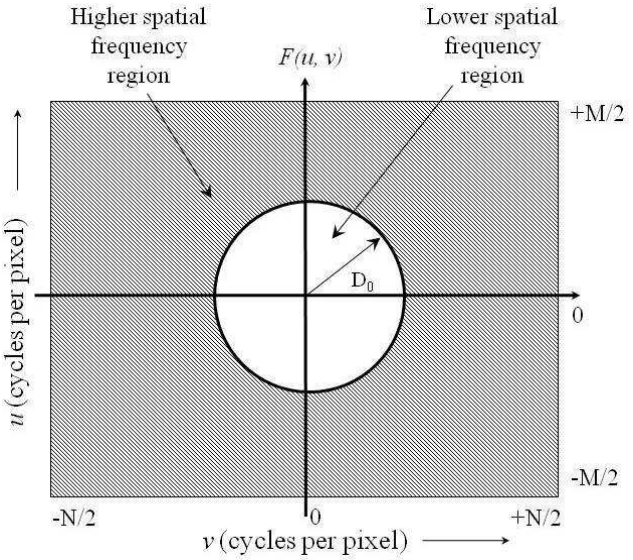

Fig 1. *The Fourier spectrum, F(u, v), of an image showing higher and lower spatial frequency regions.*

$$\text{RHFP} = \frac{\text{HFP value on pathology side} - \text{corresponding HFP value on contralateral side}}{\text{corresponding HFP value on contralateral side}} \tag{6}$$

The details of the calculation of HFP and RHFP values for cerebral infarct, ICH and brain tumor subjects are elaborated in our earlier studies [17, 18, 19], respectively.

2.3. Probability Neural Network

PNNs predominantly classifiers, are a special form of RBF network that can map any input pattern to a number of classifications. The RBF network [20] is a special class of multilayer feedforward networks, in which each unit in the hidden layer employs a RBF, such as a Gaussian kernel, as the activation function. The RBF is centered at the point specified by the weight vector associated with the unit. Both the positions and the widths of these kernels must be learned from training patterns. Each output unit implements a linear combination of these RBFs. Therefore, in a RBF network one hidden layer uses neurons with RBF activation functions and one output node is used to combine linearly the outputs of the hidden neurons.

In the present work we have chosen a basic Matlab PNN [21] for its simple structure and training manner. The most important advantage of PNN is that training is easy and instantaneous. Weights are not trained but assigned. Existing weights are never alternated, but only new vectors are inserted into weight matrices while training. Further, since the training and running procedure can be implemented by matrix manipulation, the speed of PNN is very fast. The PNN classifies input vector into a specific class, which has the maximum probability of being correct. The network architecture of a PNN implemented in the present work is shown in Fig. 2.

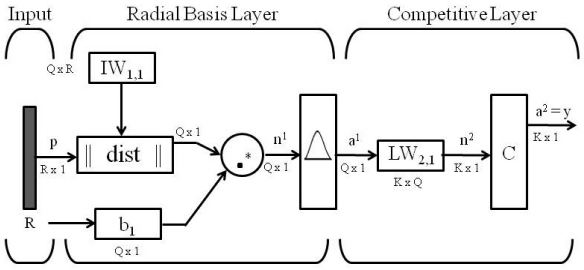

Fig 2. *PNN network architecture [21].*

(Note: The symbols and notations are adopted as used by MATLAB Neural Network Toolbox [21]. Dimensions of arrays are marked under their names)

The PNN employed in the present work has three layers: the *Input Layer*, *Radial Basis Layer* and the *Competitive Layer*. It is assumed that there are Q input vector/target vector pairs, with each target vector having K elements. Each input vector is associated with one of K classes. The dimension of the input vector (p) is R x 1. In radial basis layer, the vector distances between input vector and the weight vector made of each row of weight matrix (W) are calculated. The weights of the radial basis layer ($IW_{1,1}$) are set to the transpose of the matrix formed from the Q training pairs (P'). When an input is presented, the ||dist|| box produces a vector whose elements indicate how close the input is to the vectors of the training set. These elements are multiplied, element by element, by the bias and sent to the *radbas* transfer function given by Eq. 7 [21].

$$radbas(\mathrm{n}) = \mathrm{e}^{-\mathrm{n}^2} \tag{7}$$

The biases are all set to 0.8326/spread, where, 'spread' is the spread value of RBF. As spread becomes larger, the designed network takes into account several nearby design vectors. An input vector close to a training vector is represented by a number close to 1 in the output vector (a^1). If an input is close to several training vectors of a single class, it is represented by several elements of a^1 that are close to 1 [21].

The weights of the competitive layer ($LW_{2,1}$) are set to the matrix of target vectors. Each vector has a 1 only in the row associated with that particular class of input, and 0's elsewhere. The competitive layer sums these contributions for each class of inputs to produce as its net output a vector of probabilities. Finally, compete transfer function picks the maximum of these probabilities, and produces a 1 for that class and a 0 for the other classes. Thus, the network classifies the input vector into a specific K class because that class has the maximum probability of being correct [21, 22].

2.4. Brain Pathology Models

Brain pathology models for the subjects with cerebral infarction, ICH and brain tumors (glioma and meningioma) using HFP parameter are developed using PNN architecture (Fig. 2). The PNN model is implemented by using MATLAB version 7.7. The data set is divided into two separate data sets – the *training data set* and the *testing data set*. The training data set is used to train the network. The testing data set is used to verify the accuracy and the effectiveness of the trained network, for the classification process. Spread is an important parameter for PNN, and the accuracy of the classification process may vary with different spread values. The task in designing a PNN thereby lies in selecting spread values for the particular classification problem. To facilitate choosing the spread value in the present work we have made use of the 'leave one out method' of cross-validation [23]. Here cross-validation is carried out using a single observation from the training sample (N) as the validation data, and the remaining observations (N-1) as the training data. The value of spread is adjusted so that the chosen data for validation from the training set is appropriately classified. The process is repeated, such that each observation in the training sample is used once as the validation data. By doing so we choose the optimal spread value, giving maximum accuracy for the given classification problem. The brain pathology models using PNN developed in the present work could help find the stage of cerebral infarction, stage of ICH, and differentiate between tumor types quantitatively, relative to the RHFP parameter as its input.

3. Results and Discussions

3.1. PNN Model for Cerebral Infarction

A block schematic diagram of the cerebral infarction classification model with RHFP parameter developed using PNN architecture (Fig. 2) is shown in Fig. 3.

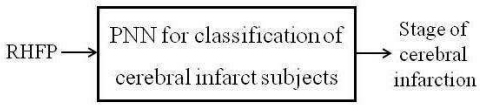

Fig 3. *Block schematic diagram of cerebral infarction classification model using RHFP.*

Studies were performed on infarct subjects to quantify the signal intensity variation distribution on DW-MR images, using RHFP values. The RHFP value evaluated from the infarct subjects was given as the input variable, and the output of the PNN block was the resulting stage of infarction for that subject. An attempt was made to associate the RHFP parameter evaluated from the infarct subjects with the different stages of infarction, by designing the PNN and training it with adequate number of input-output patterns. A total number of 65 data sets (split into different stages of infarction as shown in Table 1) were used for training the PNN. Similarly, a total number of 33 data sets (split into different stages of infarction as shown in Table 1) were used for testing the PNN. The spread value of the RBF was used as a smoothing factor and the classifier accuracy was examined with different values of spread. The optimal spread value for the classification of infarct subjects using RHFP parameter was found to be 5.

The performance of the classification model was evaluated as the percentage of the total number of patterns in the testing data set that were correctly classified. The number of data sets used for training, testing and the percentage of correct classification obtained from the PNN model, shown in Fig. 3, is tabulated in Table 1. It is observed from Table 1 that the PNN model for cerebral infarction using RHFP parameter was able to classify clearly (100%) the infarct subjects in the stages 1, 3, 4 and 5. The performance of the model for stage 2 could be improved by training with more number of corresponding input patterns. The developed PNN model could thereby aid in automatically classifying the stages of cerebral infarction, quantitatively, using RHFP measurements.

Table 1. *Number of data sets used for training, testing, and the number of correct classification obtained for tested data using cerebral infarct classification model with RHFP.*

Cerebral infarction stage (days)	Number of data sets used for training	Number of data sets used for testing	Percentage of correct classification
Stage 1 (<1)	16	8	100
Stage 2 (1 – 4)	9	6	83.33
Stage 3 (5 – 9)	26	12	100
Stage 4 (10 – 14)	8	4	100
Stage 5 (>15)	6	3	100

3.2. PNN Model for ICH

A block schematic diagram of the ICH classification model with RHFP parameter developed using PNN architecture (Fig. 2) is shown in Fig. 4.

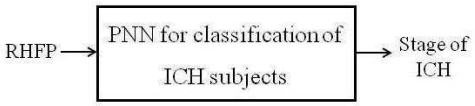

Fig 4. *Block schematic diagram of ICH classification model using RHFP.*

Studies were performed on ICH subjects to quantify the signal intensity variation distribution on DW-MR images, using RHFP parameter. The RHFP value evaluated from the ICH subjects was given as the input variable, and the output of the PNN block was the resulting stage of ICH for that subject. An attempt was made to associate the RHFP parameter evaluated from the ICH subjects with the different stages of ICH, by designing the PNN and training with adequate number of input-output patterns. A total number of 28 data sets (split into different stages of ICH as shown in Table 2) were used for training the PNN. Similarly, a total number of 14 data sets (split into different stages of ICH as shown in Table 2) were used for testing the PNN. The spread value of the RBF was used as a smoothing factor and classifier accuracy was examined with different values of spread. The optimal spread value for the classification of ICH subjects using RHFP parameter was found to be 5.

The performance of the classification model was evaluated as the percentage of the total number of patterns in the testing data set that were correctly classified. The number of data sets used for training, testing and the percentage of correct classification obtained from the PNN model, shown in Fig. 4, is tabulated in Table 2. It is observed from Table 2 that the PNN model for ICH using RHFP parameter was able to classify clearly (100%) the ICH subjects in all the stages of ICH. The developed PNN model could thereby help in classifying the stages of ICH, quantitatively, using RHFP measurements.

Table 2. *Number of data sets used for training, testing, and the number of correct classification obtained for tested data using ICH classification model with RHFP.*

ICH stage (days)	Number of data sets used for training	Number of data sets used for testing	Percentage of correct classification
Hyperacute stage (< 1)	6	3	100
Acute stage (1 – 7)	3	2	100
Late subacute stage (7 – 14)	10	5	100
Chronic stage (>14)	9	4	100

3.3. PNN Model for Brain Tumor

A block schematic diagram of the brain tumor classification model with RHFP parameter developed using PNN architecture (Fig. 2) is shown in Fig. 5.

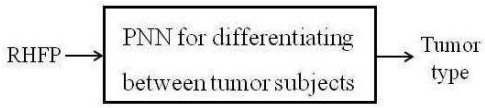

Fig 5. *Block schematic diagram of brain tumor classification model using RHFP.*

Studies were performed on the subjects with glioma and meningioma to quantify the signal intensity variation distribution on DW-MR images, using RHFP parameter. The RHFP value evaluated from the tumor subjects was given as the input variable, and the output of the PNN block was the resulting type of tumor, i.e. either glioma or meningioma. An attempt was made to associate the RHFP parameter evaluated from the tumor subjects, with the appropriate tumor type, by designing a PNN and training with adequate number of input-output patterns. A total number of 15 data sets with glioma and 08 data sets with meningioma were used for training the PNN. Similarly, a total number of 07 data sets with glioma and 04 data sets with meningioma were used for testing the PNN. The spread value of the RBF was used as a smoothing factor and classifier accuracy was

examined with different values of spread. The optimal spread value for the classification of brain tumor subjects using RHFP parameter was found to be 5.

The performance of the classification model was evaluated as the percentage of the total number of patterns in the testing data set that were correctly classified. The number of data sets used for training, testing and the percentage of correct classification obtained from the PNN model, shown in Fig. 5, is tabulated in Table 3. It is observed from Table 3 that the PNN model for brain tumor classification is able to differentiate clearly (100%) the subjects with gliomas and meningiomas. The developed PNN model could thereby help in the differential diagnosis of brain tumors, quantitatively, using RHFP measurements.

Table 3. *Number of data sets used for training, testing, and the number of correct classification obtained for tested data using brain tumor classification model with RHFP.*

Tumor type	Number of data sets used for training	Number of data sets used for testing	Percentage of correct classification
Glioma	15	7	100
Meningioma	8	4	100

4. Conclusion

The PNN model developed for cerebral infarction using RHFP values was able to quantitatively classify the infarct subjects from the normal subjects. The model presented an overall efficiency of 96.67% in categorizing the infarct subjects into their respective stages. The PNN model developed for ICH using RHFP values was able to quantitatively classify the ICH subjects from the normal subjects, and could accurately (100%) categorize the ICH subjects into their respective stages. Further, the PNN model developed for brain tumor using RHFP values was able to quantitatively classify the subjects with glioma and meningioma, from the normal subjects, and clearly differentiate (100%) between the two tumor types. The developed PNN models could thereby positively aid in the speedy and accurate radiological diagnosis of the subjects with these brain tissue pathologies, and be helpful in providing treatment at the appropriate time. Therefore, the results in our study signify that the adoption of the proposed PNN models in the clinical diagnosis could be supportive and instructive in the progression and treatment of these brain pathologies. This could positively assist the medical personnel to consider early remedial methods in order to prevent the subjects from additional damage to the brain tissue.

Acknowledgements

The authors would like to thank Dr. Sudhir Pai (Sr. Consultant, Neurosurgeon, Vikram Hospital, Bangalore, India) for his valuable assistance in data collection and Dr. Deepak Y. S. (Consultant Radiologist, Bangalore, India) for his helpful and constructive suggestions during the planning and development of this research work.

References

[1] M. V. Kumar and S. Kulkarni, "Tumors classification using PNN methods," International Journal of Soft Computing and Engineering, November 2012, 2(5), pp. 266-268.

[2] K. Z. Mao, K. C. Tan, W. Ser, "Probabilistic neural network structure determination for pattern classification," IEEE Transactions on Neural Networks, July 2000, 11(4), pp. 1009-1016.

[3] D. F. Specht, "Probabilistic neural networks," Neural Networks, 1990, 3, pp. 109-118.

[4] C. Kramer, B. Mckay, J. Belina, "Probabilistic neural network array architecture for ECG classification," Proceedings of Annual International Conference of IEEE Engineering in Medicine and Biology Society, 1995, 17, pp. 807-808.

[5] M. T. Musavi, K. H. Chan, D. M. Hummels, K. Kalantri, "On the generalization ability of neural network classifier," IEEE Transactions on Pattern Analysis and Machine Intelligence, 1994, 16(6), pp. 659-663.

[6] I. M. M. El Emary and S. Ramakrishnan, "On the application of various probabilistic neural networks in solving different pattern classification problems," World Applied Sciences Journal, 2008, 4 (6), pp. 772-780.

[7] J. M. Shen, X. W. Xia, W. G. Kang, J. J. Yuan, L. Sheng, "The use of MRI apparent diffusion coefficient (ADC) in monitoring the development of brain infarction", BMC Medical Imaging, 2011, 11(2).

[8] W. G. Bradley Jr., "MR appearance of hemorrhage in the brain," Radiology, October 1993, 189(1), pp. 15-26.

[9] R. Rajeshkannan, S. Moorthy, K. P. Sreekumar, R. Rupa, N. K. Prabhu, "Clinical applications of diffusion weighted MR imaging: A review," Indian Journal of Radiology and Imaging, 2006, 16(4), pp. 705-710.

[10] D. Le Bihan, Temperature imaging by NMR. In: Le Bihan, ed. "Diffusion and perfusion magnetic resonance: Applications to functional MRI", New York: Raven, 1995, pp. 181-187.

[11] J. H. Burdette, P. E. Ricci, N. Petitti, A. D. Elster, "Cerebral infarction: Time course of signal intensity changes on diffusion weighted images," American Journal of Roentgenology, September 1998, 171(3), pp. 791-795.

[12] J. D. Eastwooda, S. T. Engelterd, J. F. MacFall, D. M. Delongc, J. M. Provenzalea, "Quantitative assessment of the time course of infarct signal intensity on diffusion-weighted images," American Journal of Neuroradiology, April 2003, 24(4), pp. 680-687.

[13] K. Kang, D. G. Na, J. W. Ryoo, H. S. Byun, H. G. Roh, Y. S. Pyeun, "Diffusion-weighted MR imaging of intracerebral haemorrhage," Korean Journal of Radiology, October-December 2001, 2(4), pp. 183-191.

[14] S. E. Maier, Y. Sun, R. V. Mulkern, "Diffusion imaging of brain tumors," NMR in Biomedicine, August 2010, 23(7), pp. 849-864.

[15] Gonzalez R. C., Wintz P., Image transforms in 'Digital Image Processing', 2nd edition, 1987, Addison-Wesley, U.S.A.

[16] K. G. Prabhu, K. M. Patil, S. Srinivasan, "Diabetic feet at risk: A new method of analysis of walking foot pressure images at different levels of neuropathy for early detection of plantar ulcers", Medical and Biological Engineering and Computing, 2001, 39, pp. 288-293.

[17] S. S. Shanbhag, G. R. Udupi, K. M. Patil, K. Ranganath, "Analysis of cerebral infarct signal intensity on diffusion-weighted MR images using frequency domain techniques," American Journal of Biomedical Engineering, 2012, 2(3), pp. 124-130.

[18] S. S. Shanbhag, G. R. Udupi, K. M. Patil, K. Ranganath, "A new method of analysing the intracerebral haemorrhage signal intensity on brain MRI images using frequency domain techniques," Journal of Biomedical Science and Engineering, 2013, 6, pp. 56-64.

[19] S. S. Shanbhag, G. R. Udupi, K. M. Patil, K. Ranganath, "A new method of analysis of brain MRI images for quantitative grading of brain tissue pathology," Proceedings of the 2011 International Conference on Biomedical Engineering and Technology, Malaysia, 4-5 June 2011, pp. 35-39.

[20] S. Haykin, "Neural networks: A comprehensive foundation," 1994, MacMillan College Publishing Co., New York.

[21] MATLAB User's Guide, "The Math Works" Inc., 1998, Natick, MA 01760-2098.

[22] P. D. Wasserman, "Advanced methods in neural computing," Van Nostrand Reinhold, 1993, New York, pp. 35-55.

[23] A. M. Molinaro, R. Simon, R. M. Pfeiffer, "Prediction error estimation: a comparison of resampling methods," Bioinformatics, 2005, 21(15), pp. 3301-3307.